

## THE POPULATION OF BzK SELECTED ULIRGs AT $z \sim 2$

E. DADDI<sup>1,2</sup>, M. DICKINSON<sup>1</sup>, R. CHARY<sup>3</sup>, A. POPE<sup>4</sup>, G. MORRISON<sup>1</sup>, D.M. ALEXANDER<sup>5</sup>, F.E. BAUER<sup>5</sup>, W.N. BRANDT<sup>6</sup>, M. GIAVALISCO<sup>7</sup>, H. FERGUSON<sup>7</sup>, K.-S. LEE<sup>7</sup>, B.D. LEHMER<sup>6</sup>, C. PAPOVICH<sup>8</sup>, A. RENZINI<sup>9</sup>

Submitted 13 May 2005; Accepted 20 July 2005

### ABSTRACT

We investigate the multi-wavelength emission of *BzK* selected star forming galaxies at  $z \sim 2$  in the Great Observatories Origins Deep Survey (GOODS) North region. Most (82%) of the sources are individually detected at  $24\mu\text{m}$  in the Spitzer MIPS imaging, and one fourth (26%) in the VLA radio data. Significant detections of the individually undetected objects are obtained through stacking in the radio, submm and X-ray domains. The typical star forming galaxy with stellar mass  $\sim 10^{11}M_{\odot}$  at  $z = 2$  is an Ultra-luminous Infrared Galaxy (ULIRG), with  $L_{\text{IR}} \sim 1\text{--}2 \times 10^{12}L_{\odot}$  and star formation rate  $SFR \approx 200\text{--}300M_{\odot}\text{yr}^{-1}$ , implying a comoving density of ULIRGs at  $z = 2$  at least 3 orders of magnitude above the local one. *SFRs* derived from the reddening corrected UV luminosities agree well, on average, with the longer wavelength estimates. The high  $24\mu\text{m}$  detection rate suggests a relatively large duty cycle for the *BzK* star forming phase, consistently with the available independent measurements of the space density of passively evolving galaxies at  $z > 1.4$ . If the IMF at  $z = 2$  is similar to the local one, and in particular is not a top-heavy IMF, this suggests that a substantial fraction of the high mass tail ( $\gtrsim 10^{11}M_{\odot}$ ) of the galaxy stellar mass function was completed by  $z \approx 1.4$ .

*Subject headings:* galaxies: evolution — galaxies: formation — cosmology: observations — galaxies: starbursts — galaxies: high-redshift

### 1. INTRODUCTION

The rate at which stars in massive galaxies were assembled is a crucial measurement for the characterization of galaxy formation. Hierarchical clustering models have traditionally favored galaxy formation at quiescent rates (e.g. Cole et al. 2001). Formation of stars at high rates in massive galaxies would qualitatively match monolithic formation scenarios (Eggen et al. 1962). Intense star formation at high redshift has been established for submm selected galaxies. These are relatively extreme objects, with space densities nearly two orders of magnitude smaller than local massive galaxies (e.g., Scott et al. 2002). Extending the census to less extreme star formation rate (*SFR*) levels is necessary, but obtaining reliable *SFR* estimates for high-redshift galaxies is a challenging endeavor. The widespread presence of dust, absorbing the light of high mass stars and re-radiating it at longer wavelengths, complicates the immediate use of the UV luminosity as a *SFR* indicator, as uncertain large corrections are required. A multi-wavelength approach, although observationally demanding, can yield more robust measures of *SFR*.

The major growth and assembly of galaxies' stellar mass is observed during the epoch between redshifts  $1 < z < 3$  (Dickinson et al. 2003; Rudnick et al. 2003). Daddi et al. (2004b), on the basis of the highly complete spectroscopic database of the K20 survey (Mignoli et al. 2005), showed that a relatively

clean, efficient and complete (reddening independent) selection of massive galaxies in the above redshift range can be obtained by selecting outliers in a  $(B - z)$  vs.  $(z - K)$  diagram. For  $z \sim 2$  objects with  $K < 20$ , selected in this way, Daddi et al. (2004a;b; hereafter D04a and D04b) derived high masses and *SFRs*, suggesting they are the progenitors of local massive spheroids caught during their phase of major assembling. The *SFRs* derived from the dust-corrected UV luminosities are however uncertain.

In this letter, we have taken advantage of the *BzK* selection to assemble a statistical sample of  $K < 20$  (Vega) massive star forming galaxy candidates at  $1.4 < z < 2.5$  in the Great Observatories Origins Deep Survey (GOODS) North field. Deep  $24\mu\text{m}$  observations, obtained with MIPS on board of the Spitzer Space Telescope (SST), were used to study their rest-frame mid-IR emission properties. Deep X-ray, submm and radio data allow us to build a panchromatic view of their spectral energy distributions (SEDs), and to shed light on their nature and star formation activity. We discuss the implications for the assembly process of massive galaxies. We use a Salpeter initial mass function (IMF) from 0.1 to  $100 M_{\odot}$ , and a WMAP cosmology with  $\Omega_{\Lambda}, \Omega_M = 0.73, 0.27$ , and  $h = H_0[\text{km s}^{-1} \text{Mpc}^{-1}]/100 = 0.71$ .

### 2. BzK SELECTION OF $z \sim 2$ GALAXIES IN GOODS-NORTH

The GOODS-North field has been observed in the *K*-band with the Flamingos camera at the Mayall 4-m NOAO telescope. About 4–7 hours integration were collected with average  $1.2''$  seeing, over each of two contiguous pointings, reaching  $5\sigma$  limits of  $K \sim 20.5$  (Vega) for point sources. Calibration was done using objects in common with 2MASS. Observations in the *B*- and *z*- bands were obtained at the Subaru telescope with Suprime-Cam with  $< 1''$  seeing, and are described in Capak et al. (2004). Sources were selected over an area of  $154 \text{ arcmin}^2$  to  $K < 20$  (Vega), thus matching the limit where the *BzK* criterion is currently calibrated by the K20 survey (D04b). The Capak et al. (2004) zeropoints were slightly adjusted, and a small color term was applied to the *B*-band

<sup>1</sup> National Optical Astronomy Observatory, 950 N. Cherry Ave., Tucson, AZ, 85719

<sup>2</sup> Spitzer Fellow; edaddi@noao.edu

<sup>3</sup> Spitzer Science Center, Caltech, MS 220-6, CA 91125

<sup>4</sup> Department of Physics & Astronomy, University of British Columbia, Vancouver, BC, V6T 1Z1, Canada

<sup>5</sup> Institute of Astronomy, Madingley Road, Cambridge CB3 0HA, UK

<sup>6</sup> Department of Astronomy and Astrophysics, 525 Davey Laboratory, Pennsylvania State University, University Park, PA 16802

<sup>7</sup> Space Telescope Science Institute, 3700 San Martin Drive, Baltimore, MD 21218

<sup>8</sup> Steward Observatory, University of Arizona, Tucson, AZ 85721

<sup>9</sup> ESO, Karl-Schwarzschild-Strasse 2, Garching 85748, Germany

magnitudes because the Subaru  $B$ -band filter is redder than the one used in D04b. 169  $z \sim 2$  star forming galaxy candidates were selected having  $BzK \equiv (z - K)_{AB} - (B - z)_{AB} > -0.2$ . We are explicitly excluding from the analysis the 13 objects with  $BzK < -0.2$  and  $(z - K)_{AB} > 2.5$  that are candidate passively evolving galaxies at  $z > 1.4$ . However, the shallower depth of the  $B$ -band data (compared to those in D04b) prevents a clean separation of  $z > 1.4$  passive and star forming galaxies among sources with the reddest  $z - K$  colors. We might expect up to 10-15 genuine passively evolving  $z > 1.4$  galaxies among the  $BzK > -0.2$  objects, counting the sources with no or low-significance  $B$ -band detection. 38/169 (22%) objects were discarded as likely AGN-dominated, because detected in the hard X-ray band (Alexander et al. 2003). The AGN contamination that we recover here is higher than in D04b, owing to the deeper X-ray data. The surface density of the 131 non X-ray bright  $BzK > -0.2$  objects in GOODS-N is  $0.85 \pm 0.07 \text{ arcmin}^{-2}$  (Poisson), consistent with that measured in the K20 survey. On the basis of the K20 survey results (D04b), we assume in the following that the 131 galaxies with  $BzK > -0.2$  are mostly at  $1.4 < z < 2.5$ , with a relatively flat redshift distribution in that interval and with a  $\lesssim 10\%$  contamination of objects at  $1 < z < 1.4$ , and that our sample is complete for star forming galaxies with  $K < 20$  at  $1.4 < z < 2.5$ . This is also supported by our photometric redshifts, and by the limited amount of spectroscopic redshift currently available for  $K < 20$ ,  $BzK$  sources in GOODS-N.

### 3. MULTI- $\lambda$ OBSERVATIONS OF $BzK$ SELECTED GALAXIES

*Rest frame UV:* The calibrations of D04b were used for estimating stellar masses, reddening and  $SFR$  of  $BzK$  selected galaxies from their observed properties in the optical/IR. The average mass of our  $z = 2$  object is  $1.0 \times 10^{11} M_{\odot}$  and the sample is complete above  $\sim 10^{11} M_{\odot}$  for  $1.4 < z < 2.5$ . The median  $B - z = 1.50$  color translates to a reddening of  $E(B - V) = 0.40$  for the Calzetti et al. (2000) law. This median reddening is similar to our estimate of the  $E(B - V)$  upper limit for the UV criteria of Steidel et al. (2004) for selecting  $z \sim 2$  galaxies, and we estimate that roughly 50% of the  $z \sim 2$   $BzK$  star forming galaxies with  $K < 20$  would be missed when selecting in the UV. We find an average  $SFR \sim 220 M_{\odot} \text{ yr}^{-1}$  for our sample, based on the estimate of the reddening corrected  $1500\text{\AA}$  rest frame luminosity, with a median (average) correction factor of 46 (118). The ratio of the averages of the corrected and uncorrected  $SFR$ s is 42.

*MIPS  $24\mu\text{m}$ :* Deep  $24\mu\text{m}$  observations of GOODS-North were obtained with SST MIPS, as a part of the GOODS Legacy Program (M. Dickinson et al., in preparation), for a total of 10.4 hours exposure time per sky pixel. Sources were detected in the  $24\mu\text{m}$  data using SST IRAC data as prior positions, in order to improve source deblending (R. Chary et al., in preparation). We cross-correlated the 131  $BzK$  selected galaxies to MIPS objects using a  $2''$  search radius (expected false matching rate of order of a few %). 107/131 (82%) of the  $z \sim 2$  galaxies are matched to a MIPS counterpart. The  $24\mu\text{m}$  flux ( $f_{24}$ ) ranges from 300-500  $\mu\text{Jy}$  for the brightest sources to the typical  $3\sigma$  limits in the range of 15-30  $\mu\text{Jy}$  (depending on position) for undetected sources. The median  $f_{24}$  is 110  $\mu\text{Jy}$ , including non detected sources. The average is 127-124  $\mu\text{Jy}$ , depending on whether for the undetected sources we use the  $3\sigma$  upper limit or assign zero flux to them. A Kendall's  $\tau$  test indicates that  $f_{24}$  correlates with the  $K$ -band flux, with a 99% level of significance. Comparing to the full GOODS-N MIPS  $24\mu\text{m}$  catalog,  $BzK$  star forming

galaxies account for about 7-10% of  $24\mu\text{m}$  selected sources above 50 to 300  $\mu\text{Jy}$ , with the fraction varying slightly with  $24\mu\text{m}$  limiting flux. These figures place lower limits to the fraction of  $z > 1.4$  galaxies in  $24\mu\text{m}$  selected galaxy samples, which are consistent with the predictions of Chary & Elbaz (2001; hereafter CE01), i.e. 16%. At  $1.4 < z < 2.5$  the  $24\mu\text{m}$  observations probe rest-frame wavelengths of 7-10  $\mu\text{m}$ , the mid-IR region dominated by strong PAH emission features and silicate absorption. In order to constrain the level of IR luminosity ( $L_{\text{IR}} \equiv L_{8-1000\mu\text{m}}$ ), hence  $SFR$ , required to reproduce the observed  $f_{24}$  levels, we used the models from CE01, which provide  $L_{\text{IR}}$ -dependent templates calibrated from the local SEDs of IR luminous galaxies. For a given  $L_{\text{IR}}$ , these models predict a factor of  $\approx 5$  decrease of  $f_{24}$  from  $z = 1.4$  to  $z = 2.5$ . Assuming a flat redshift distribution within  $1.4 < z < 2.5$  for the  $BzK > -0.2$  selected galaxies, models with  $L_{\text{IR}} = 1.7 \times 10^{12} L_{\odot}$  are required to reproduce the 125  $\mu\text{Jy}$  average flux level<sup>1</sup>. This corresponds to an average  $SFR \sim 300 M_{\odot} \text{ yr}^{-1}$  (Kennicutt et al. 1998). Using instead the empirical SED of Arp 220, calibrated by ISO observations of the PAH features region, one would expect a relative  $f_{24}$  peak around  $z \sim 2$  and minima toward  $z = 1.4$  and  $z = 2.5$ . This is due to strong 9.7  $\mu\text{m}$  silicate absorption, a feature which has been observed to be quite common at  $z \sim 2$  in sources with  $L_{\text{IR}} \gtrsim 10^{13} L_{\odot}$  (e.g., Yan et al. 2005). The  $f_{24}$  expected from Arp 220 when averaged within  $1.4 < z < 2.5$  is about 30  $\mu\text{Jy}$ . For the Arp 220 IR luminosity of  $1.5 \times 10^{12} L_{\odot}$ , this in turn implies  $L_{\text{IR}} \sim 6 \times 10^{12} L_{\odot}$  for the typical  $BzK$  star forming galaxy at  $z = 2$ , or very large  $SFR \sim 1000 M_{\odot} \text{ yr}^{-1}$  (this high value is disfavored by the other measurements, see below).

*Radio 20cm:* 34/131 (26%) of the  $BzK > -0.2$  galaxies are individually detected with  $S/N > 3$  in deep VLA radio data (Richards 2000; reprocessed by G. Morrison et al., in preparation), with fluxes at 1.4 GHz in the range of 20-160  $\mu\text{Jy}$  (when excluding a radio galaxy with 1 mJy flux), and an average of 37  $\mu\text{Jy}$ . Stacking of the 94 undetected sources<sup>2</sup>, after discarding 3 objects close to unrelated radio sources, yields a  $S/N = 8$  detection for an estimated average flux density of  $10 \pm 2 \mu\text{Jy}$ . When adding to this the individual detections we derive an average flux density of about 17  $\mu\text{Jy}$  for the full sample of 131 objects. Using a radio spectral index  $\alpha = -0.8$  ( $f_{\nu} \propto \nu^{-\alpha}$ ) we derive a luminosity of  $3.6 \times 10^{23} \text{ W Hz}^{-1}$  for an average  $\langle z \rangle = 1.9$ , which implies  $L_{\text{IR}} \sim 1.2 \times 10^{12} L_{\odot}$  and  $SFR \sim 210 M_{\odot} \text{ yr}^{-1}$  (Yun et al. 2001; Kennicutt et al. 1998).

*SCUBA  $850\mu\text{m}$ :* Only one of the 131 sources appears in the list of Pope et al. (2005) with a flux of 4 mJy. In order to estimate the average  $850\mu\text{m}$  flux of the undetected objects we used the Borys et al. (2003) HDF-N SCUBA supermap. Some 97 MIPS-detected objects were stacked<sup>3</sup>, after excluding those separated by less than a SCUBA beam halfwidth ( $7''$ ) from any known SCUBA detection. As the

<sup>1</sup> Note that we are studying the  $24\mu\text{m}$  properties of a near-IR selected sample of galaxies, not a  $24\mu\text{m}$  selected sample. Its redshift distribution is expected to be flat within  $1.4 < z < 2.5$ , independent of the behavior of the  $24\mu\text{m}$  flux with redshift. As we are detecting 82% of the objects, the typical flux that we detect corresponds to the source at typical redshift.

<sup>2</sup> To stack the radio data, sub images were extracted at the locations of the non-detected sources. These were corrected for VLA primary beam attenuation and combined using a weighted average. The integrated flux density and error were computed with the AIPS task JMFIT, which modeled the stacked emission using an elliptical Gaussian.

<sup>3</sup> We are using only MIPS-detected objects to maximize the signal to noise by avoiding passive galaxy contaminants, while the possible star forming galaxy contaminants at  $1 < z < 1.4$  would not alter significantly the stacking because of the mild dependence between  $850\mu\text{m}$  flux with redshift.

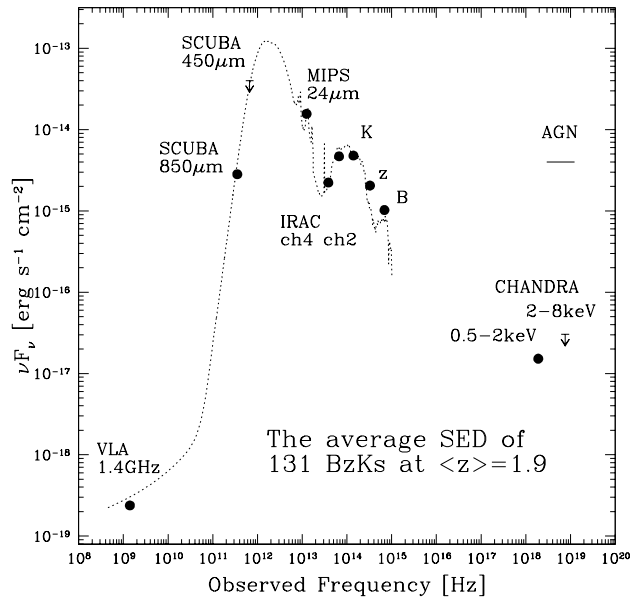


FIG. 1.— The average multi-wavelength emission of 131 *BzK* selected star forming galaxies at  $1.4 < z < 2.5$ . The model shown here (from CE01) has  $L_{\text{IR}} = 1.7 \times 10^{12} L_{\odot}$  and is redshifted to  $z = 1.9$ . Measurements in SST IRAC ch2 ( $4.5\mu\text{m}$ ,  $AB = 20.78$  mag) and ch4 ( $8.0\mu\text{m}$ ,  $AB = 20.99$  mag) were obtained from the data of M. Dickinson et al., in preparation. The horizontal bar on the right shows the 2–8 keV emission that would be expected from a typical AGN having the mid-IR flux observed for our objects.

depth of the SCUBA data vary considerably over GOODS-N, we used weights in the stacking based on the local noise. The average  $850\mu\text{m}$  signal is  $1.0 \pm 0.2\text{mJy}$ . We checked that this 5-sigma detection is robust using Monte-Carlo simulations. Scaling down the result by 18% to account for the MIPS undetected objects, the average  $850\mu\text{m}$  flux corresponds to  $L_{\text{IR}} \sim 1.0 \times 10^{12} L_{\odot}$ , both for the CE01 templates and when using Arp 220, or to  $SFR \sim 170 M_{\odot}\text{yr}^{-1}$ . At  $450\mu\text{m}$  we obtain a  $3\sigma$  upper limit of  $6\text{mJy}$ , consistent with the models.

*Chandra soft and hard X-rays:* Is the detected IR emission AGN or starburst powered? At  $z \sim 2$  the Chandra hard 2–8 keV band is sensitive to highly penetrating rest-frame X-rays up to about 20 keV, which can escape large column densities up to about  $10^{24} \text{cm}^{-2}$ . The lack of hard X-ray detection in the Chandra 2 Ms exposure should ensure that bright AGNs are generally not included in our sample. The typical upper limits to the 2–8 keV flux of order  $< 3 \times 10^{-16} \text{erg s}^{-1} \text{cm}^{-2}$  coupled to the typical  $24\mu\text{m}$  fluxes measured, imply lower limits to the  $24\mu\text{m}$  to 2–8 keV flux ratios, for single objects, about one full order of magnitude larger than expected from AGNs (see e.g. Rigby et al 2004). This suggests that the  $24\mu\text{m}$  emission in our sample is powered by star formation in most cases. While we have discarded all direct hard X-ray detections from our sample, 6/131 (4.5%) of the objects are detected in the soft-band only, with fluxes  $\lesssim 10^{-16} \text{erg s}^{-1} \text{cm}^{-2}$  (Alexander et al. 2003). Four of these are detected also in the radio, and one is the only SCUBA detection. These soft sources are most likely the most extreme starbursts in the  $BzK > -0.2$  sample, similar to object ID#5 described in D04a. We stacked the X-ray undetected sources, considering only the GOODS-N region within 6 arcmin of the 2 Ms Chandra data aim point where the sensitivity is the highest, and avoiding all objects closer than 3 Chandra PSF from known X-ray sources. The stacked images result

in a  $8.5\sigma$  detection in the soft 0.5–2 keV band, for a flux of  $1.0 \times 10^{-17} \text{erg s}^{-1} \text{cm}^{-2}$ . The non detection in the hard 2–8 keV band constrains the photon spectral index  $\Gamma > 1.0$  at the 3-sigma level, and implies an average  $24\mu\text{m}$  to 2–8 keV flux ratio over two orders of magnitude above what is typical for AGN at  $z \sim 2$  (Rigby et al. 2004). If AGN are present they would have to be heavily Compton thick. Using  $\Gamma = 2.0$  as appropriate for starbursts implies a rest-frame luminosity in the 2–10 keV range of  $3.4 \times 10^{41} \text{erg s}^{-1}$  for  $\langle z \rangle = 1.9$ . Adding back the individual soft X-ray detections would increase the 2–10 keV luminosity to about  $5 \times 10^{41} \text{erg s}^{-1}$ . This is a factor of two lower than estimated by D04b for K20 *BzK* sources. Using the Ranalli et al. (2003) calibration this translates into an average  $SFR \sim 100 M_{\odot}\text{yr}^{-1}$ , or  $SFR \sim 500 M_{\odot}\text{yr}^{-1}$  if using the Persic et al. (2004) calibration. The large difference is due to the relative expected importance of high versus low mass X-ray binaries. The latter calibration appears more appropriate when dealing with IR luminous sources with  $L_{\text{IR}} \gtrsim 10^{12} L_{\odot}$  (Persic et al. 2004).

#### 4. DISCUSSION

The multi-wavelength SED (Fig. 1) of *BzK* selected  $z = 2$  star forming galaxies consistently indicates an average  $L_{\text{IR}} \sim 1\text{--}2 \times 10^{12} L_{\odot}$  and  $SFR \sim 200\text{--}300 M_{\odot}\text{yr}^{-1}$ , supporting the earlier claims of D04a;b and implying that the local correlations (e.g., the mid and far-IR to radio correlations) hold, for the average *BzK* galaxy, also at  $z \approx 2$ . While the X-ray based estimate appears the least accurate, due mainly to the large uncertainties in its calibration, the X-ray properties clearly support that the mid to far-IR emission of these sources is indeed dominated by vigorous star formation and not by nuclear activity. The inferred average  $L_{\text{IR}} \gtrsim 10^{12} L_{\odot}$  implies that the typical *BzK* selected star forming galaxy is an Ultra Luminous IR Galaxy (ULIRG). Morphology from HST ACS indeed suggests that, in many cases, these  $z = 2$  galaxies are assembling through merging (D04a), similarly to local ULIRGs. Using the volume at  $1.4 < z < 2.5$  ( $5.7 \times 10^5 \text{Mpc}^3$ ), we can put a lower limit to the spatial density of ULIRGs at  $z \sim 2$  of about  $1\text{--}2 \times 10^{-4} \text{Mpc}^{-3}$ . This is about 3 orders of magnitude higher than at  $z \sim 0.1$  (Sanders et al. 2003), and a factor of 2–3 higher than at  $z = 1$  (Le Flocc’h et al. 2005). While ULIRGs are exceptional objects for the local universe, they appear to be the norm among massive  $z \approx 2$  star forming galaxies.

From the X-ray we also derive a fairly low X-ray to optical flux ratio of  $\log(f_{0.5\text{--}2 \text{keV}}/f_{\text{R}}) \sim -1.7$ , which suggests that also the rest frame UV emission of these  $z = 2$  galaxies is dominated by the emission of stars. The average  $SFR$  inferred from the dust-corrected UV luminosity agrees well with the longer wavelength estimates. Fig. 2 (top) shows the ratio of  $24\mu\text{m}$  to *B*-band flux densities as a function of the rest-frame UV galaxy colors. Apart from *K*-correction effects, this observed mid-IR to UV luminosity ratio measures the ratio of dust-extinguished to relatively unobscured  $SFR$ . The Kendall’s  $\tau$  test detects a correlation at  $> 99.9$  confidence level. A similar trend is found when using the radio flux instead of  $f_{24}$ . This confirms that, in general, the red UV continua of *BzK* selected  $z = 2$  star forming galaxies are indeed due to dust reddening. The diagonal line plotted in Fig. 2 (top) shows the expected scaling in the case that the UV and mid-IR trace the same amount of  $SFR$ . The average ratio and its dependence with the UV color are in line with what is expected. Sources with higher  $24\mu\text{m}$  flux, however, tend to have systematically larger ratios, and vice-versa. This can be more clearly seen in Fig. 2 (bottom), where we plot the  $24\mu\text{m}$  to

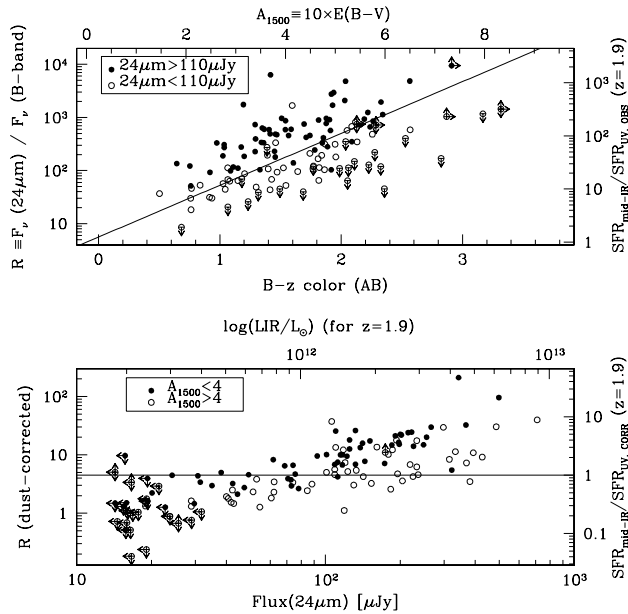


FIG. 2.— (Top panel). The ratio of  $24\mu\text{m}$  to B-band flux for  $K < 20$   $BzK$  selected  $z = 2$  star forming galaxies in GOODS-North as a function of  $B-z$  color (i.e. dust extinction at  $1500\text{\AA}$ , as inferred using a Calzetti et al. 2000 law). The diagonal line shows the expected ratio for the average  $z = 1.9$  in the case that the UV and mid-IR trace the same amount of star formation. Solid and empty symbols are for sources with  $f_{24}$  above or below the median, respectively. (Bottom panel). The dust extinction corrected  $24\mu\text{m}$  to B-band flux ratio, as a function of the  $24\mu\text{m}$  flux. Solid and empty symbols are for sources with UV reddening below or above the median, respectively. In both panels, values on axis labeled with  $L_{\text{IR}}$  or  $\text{SFR}$  are for an average  $z = 1.9$  and were computed using the CE01 model reproducing the average SED (Fig 1).

$B$ -band flux ratio (with the  $B$ -band flux here being corrected for dust reddening) as a function of the  $24\mu\text{m}$  flux: a clear trend with  $24\mu\text{m}$  flux is present. The expected K-correction term is small, and this plot suggests that sources with higher  $L_{\text{IR}}$  have progressively larger fractions of the  $\text{SFR}$  that cannot be recovered from the UV luminosity even after correcting for dust reddening. However, such a strong trend is not reproduced using the radio data for the radio detected objects. Fig. 2 (bottom) also shows that, at fixed  $f_{24}$ , the sources with bluer UV continua tend to have higher corrected  $24\mu\text{m}$  to  $B$ -band flux ratio by a factor of 2 on average.

Vigorous starbursts are present within the  $BzK$  selected star forming galaxies at  $z = 2$ , which have also fairly large typical stellar masses of  $\sim 10^{11}M_{\odot}$  for  $K < 20$  (Vega). These masses would grow even larger as a result of star formation, depending on the duty cycle of the star formation event. The high detection rate (82%) at  $24\mu\text{m}$  supports the possibility that high

$\text{SFR}$ s among these  $K < 20$  sources are sustained for a substantially long amount of time during  $1.4 < z < 2.5$ . When limiting to a common stellar mass threshold, e.g.  $\gtrsim 10^{11}M_{\odot}$ , the space densities of passively evolving galaxies is comparable to that of vigorous starbursts within  $1.4 < z < 2$ , and perhaps much smaller at  $2 < z < 2.5$  (Daddi et al. 2005; Kong et al. 2005; McCarthy et al. 2004). This would suggest that the average duty cycle is at least 50%, and likely more. The Universe ages from 2.6 Gyr to 4.6 Gyr between  $z = 2.5$  and 1.4, and about 1 Gyr is still available on average per galaxy before  $z = 1.4$ , implying a continuation of the star formation event for order 0.5 Gyr or more, on average, and that typically these objects have been active for a similar or larger amount of time before observations. This is also consistent with the typical age of the present SF event inferred from the optical/IR SED fitting with constant star formation rate models, which is mainly based on the strength of the observed Balmer break (about 0.7 Gyr; D04a; see also Shapley et al. 2005). Therefore, by  $z = 1.4$  the typical mass of these galaxies will have roughly doubled, reaching  $\sim 2 \times 10^{11}M_{\odot}$ , on average. From their observed space densities ( $\sim 2.3 \times 10^{-4} \text{Mpc}^{-3}$ ) and  $\text{SFR}$ s, we infer that the integrated stellar mass density formed within  $BzK > -0.2$  galaxies with  $K < 20$  in the 2 Gyr time within  $1.4 < z < 2.5$  is  $\sim 10^8 M_{\odot} \text{Mpc}^{-3}$ , independent of the duty cycle. This is only  $\sim 20\%$  of the local total stellar mass density, but is comparable to the local stellar mass density for objects with stellar mass  $> 2 \times 10^{11}M_{\odot}$  (Cole et al. 2001). If the IMF at  $z = 2$  is similar to the local one, and in particular is not a top-heavy IMF, this suggests that by  $z \approx 1.4$  the assembly of the high-mass tail ( $> 10^{11}M_{\odot}$ ) of present day's galaxies mass function was, in a significant part, completed. This is also supported by the measurements, quoted above, of a comparable space densities of old and passive galaxies with similar masses to the star-forming  $BzK$ s already existing at  $1.4 < z < 2$ , and with the evidences (Papovich et al. 2005) of strongly declining specific  $\text{SFR}$ s for  $z < 1.4$  massive galaxies.

We thank the many other members of the GOODS team who have helped to make these observations possible. We are grateful to Colin Borys for his work on the HDF-N SCUBA supermap and to the anonymous referee and to the editor, John Scalo, for useful comments. ED gratefully acknowledges NASA support through the Spitzer Fellowship Program, award 1268429. Support for this work, part of the Spitzer Space Telescope Legacy Science Program, was provided by NASA through Contract Number 1224666 issued by the JPL, Caltech, under NASA contract 1407.

## REFERENCES

- Borys C., Chapman S., Halpern M., Scott D., 2003, MNRAS, 344, 385  
 Calzetti D., Armus L., Bohlin R. C., et al., 2000, ApJ, 533, 682  
 Capak P., et al., 2004, AJ, 127, 180  
 Chary R., Elbaz D., 2001, ApJ, 556, 562 (CE01)  
 Cole S., et al., 2000, MNRAS, 319, 168  
 Cole, S., Norberg, P., Baugh, C. M., et al., 2001, MNRAS, 326, 255  
 Daddi E., Cimatti A., Renzini A., et al., 2004a, ApJ, 600, L127 (D04a)  
 Daddi E., Cimatti A., Renzini A., et al., 2004b, ApJ, 617, 746 (D04b)  
 Daddi E., et al., 2005, ApJ, 626, 680  
 Dickinson M., Papovich C., Ferguson H. C., Budavári T., 2003, ApJ, 587, 25  
 Eggen O. J., Lynden-Bell D., Sandage A. R., 1962, ApJ, 136, 748  
 Kennicutt R. C., 1998, ARA&A, 36, 189  
 Kong X., Daddi E., Arimoto N., et al., 2005, ApJ, submitted  
 Le Floch E., et al., 2005, ApJ in press (astro-ph/0506462)  
 McCarthy P. J., et al., 2004, ApJ, 614, L9  
 Mignoli M., et al., 2005, A&A, 437, 883  
 Papovich C., et al., 2005, submitted to ApJ  
 Persic M., Rephaeli Y., Braitov V., et al., 2004, A&A, 419, 849  
 Pope A., Borys C., Scott D., et al., 2005, MNRAS, 358, 149  
 Ranalli P., Comastri A., Setti G., 2003, A&A, 399, 39  
 Rigby J. R., et al., 2004, ApJS, 154, 160  
 Richards E. A., 2000, ApJ, 533, 611  
 Rudnick, G., et al. 2003, ApJ, 599, 847  
 Sanders D. B., Mazzarella J. M., Kim D.-C., et al., 2003, AJ, 126, 1607  
 Scott S. E., et al., 2002, MNRAS, 331, 817  
 Shapley A., et al., 2005, ApJ, 626, 698  
 Steidel, C. C., Shapley, A. E., Pettini, et al., 2004, ApJ, 604, 534  
 Yan L., Chary R., Armus L., et al., 2005, ApJ in press (astro-ph/0504336)